

# Frequency Spectrum Analysis of Magnetic Field Strength for Effective Condition Monitoring of Magnetic Cores

Hamed Hamzehbahmani, *Senior member, IEEE*  
Department of Engineering, Durham University, Durham, DH1 3LE, UK

**Abstract-** Fault diagnosis and condition monitoring of electromagnetic devices is a normal practice to prevent unpredicted downtime and catastrophic failure. As a key objective in effective fault diagnostic, quality assessment of magnetic cores to identify core faults or Interlaminar Faults (ILFs) can be addressed. ILFs in magnetic cores make direct impact on the magnetising process, which results in anomaly and asymmetry in the magnetic fields and hence magnetising currents. This paper presents a pragmatic approach for ILF analysis and condition monitoring of magnetic cores with Grain-Oriented Electrical Steels (GOES). The proposed technique relies on interpreting frequency spectrum of the magnetic field over one cycle of magnetisation. To this end, experimental work was undertaken on stacks of four standard Epstein size laminations subjected to artificial ILFs of different severity. Impacts of each fault scenario on dynamic hysteresis loop (DHL), and instantaneous wave shapes of magnetic field strength in time and frequency domains were studied. This work found that frequency spectrum analysis of magnetic field strength could be employed as a diagnostic tool to identify ILF. This approach can effectively increase accuracy of fault diagnosis and improve detectability of weak fault signatures.

**Index Terms:** Condition monitoring, electromagnetic device, core fault, Interlaminar fault, grain-oriented electrical steels, dynamic hysteresis loop, magnetic field, frequency spectrum.

## I. INTRODUCTION

ELECTROMAGNETIC devices, i.e., e-machines, transformers, and reactors, are the key players in the accelerating trend toward the Net Zero target. Electromagnetic devices with advanced performance and enhanced efficiency are essential to pioneer sustainable operation of the power systems and energy security. Working principle and energy conversion process of all kinds of electromagnetic devices of any size relies on the distinct aspect of the magnetic hysteresis. Therefore, a comprehensive analysis on physical mechanism of the magnetic hysteresis has a notable impact on optimised design and operation of electromagnetic devices to boost the clean energy production.

Manufacturing process of electromagnetic devices usually starts with their magnetic cores, which are constructed from electrical steel laminations. Like other parts of the device, magnetic cores can experience variety of faults which are known as core faults or Interlaminar Faults (ILFs) [1-2]. ILFs can create fault current loops, which deteriorate the laminated structure of the magnetic cores. Local hot spot and local power loss are the immediate consequences of core faults, that impact on the normal operation and overall efficiency of the device [3]. Perspective view of a stack of laminations subjected to ILF, and formation of the corresponding fault current in the short circuit zone are schematically shown in Figs 1-a and 1-b, respectively.

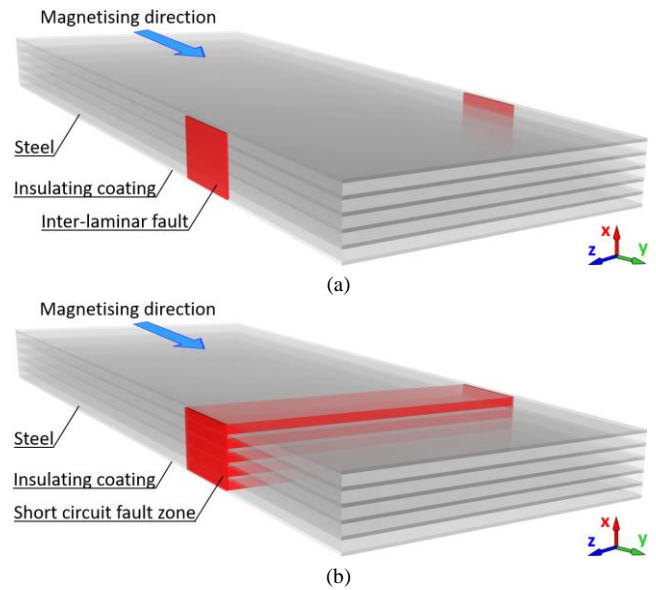


Fig 1 (a) Stack of laminations subjected to ILF, (b) formation of the corresponding fault current in the short circuit zone

ILF problem can start with minor undetected faults that could potentially cause progressive degradation in the insulating coating of the laminations and end up with major faults. If not detected in a timely manner, this phenomenon will continue until a total machine breakdown. Examples of core fault in magnetic core of a 50 MVA, 110 kV power transformer core [4], and fault in the stator core of an electric motor due to winding arcing are shown in Figs 2-a and 2-b, respectively.

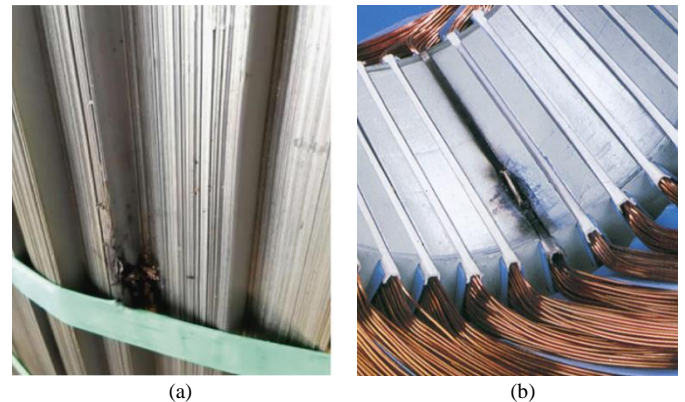


Fig 2 (a) Core fault in magnetic core of a 50 MVA, 110 kV power transformer [4], and (b) Stator core fault due to winding arcing in the slot

The procedure of monitoring and processing operational parameters of electromagnetic devices for fault identification and failure prediction are known as fault diagnosis and condition

monitoring. To this end, identifying core faults is a major goal with a significant role to play in the entire process. Accurate fault diagnosis at early stage via effective condition monitoring techniques is crucial to ensure continuous operation of e-machines and sustainable energy delivery, specifically for strategically important applications. With such systems in place, unexpected downtime, catastrophic failing, and risk to the operators can be avoided [5].

Following decades of research and development, effective techniques of condition assessment of e-machines and other types of electromagnetic devices have been developed, and commercially available for the end users. Depend on the fault types and diagnostic objectives, different approaches can be designed and executed for condition monitoring. Nevertheless, the overall procedure relies on measuring and monitoring certain operational parameters, e.g., power loss, temperature, magnetic field, vibration, etc. [6-7]. Data analysis and signal processing techniques are then implemented to catalogue and convert this data into meaningful information that can be used to classify and fault diagnosis purposes [8-9]. This is in line with the guiding principles and definition of condition monitoring [10].

When the concern is quality of the magnetic cores, e.g., transformer cores, no-load test to measure magnetic loss is a normal practice to evaluate overall quality of the concerned cores. This test is extensively implemented in the manufacturing sites for quality assessment of brand-new transformers, and for power transformers in operations during the routine and type tests. However, this test as defined in the British standard BS EN 60076-1-2011 [11], is mainly to measure overall power loss of the magnetic cores and does not grant details of the power loss distribution and magnetising processes.

In recent publications the author developed analytical and experimental techniques for fault diagnosis and condition monitoring of magnetic cores based on the phenomenology of magnetic hysteresis [1-3]. These techniques rely on measuring and interpreting the dynamic hysteresis loops (DHLs) and instantaneous waveform of the magnetic fields in time domain. This paper aims to propose a new pragmatic approach for fault diagnosis and condition monitoring of magnetic cores by looking at the frequency spectrum of the magnetic field strength. The proposed approach and associated analysis are built on the previous knowledge of impacts of core faults on magnetising processes of the magnetic cores and expand this analysis from time domain into frequency domain. A key feature of this study is to increase accuracy of fault diagnosis to improve detectability of weak fault signature. For this purpose, experimental work was conducted on stacks of standard Epstein size laminations of Grain Oriented Electrical Steels (GOES). Artificial ILFs, with a wide range of severity level, were applied between the laminations. DHLs and instantaneous waveshapes of magnetic field strength of the test samples were acquired. As the main contribution of the work, an in-depth analysis on the acquired data in time and frequency domains were performed to understand impacts of ILFs on frequency spectrum of magnetic field strength. The proposed technique and associated analysis can provide new prospect in condition monitoring of magnetic cores of practical electromagnetic devices.

## II. THEORETICAL CONTEXT OF ENERGY LOSS MECHANISM OF GOES:

Magnetic hysteresis and its phenomenological concepts grant a solid ground to comprehend dynamic performance and energy loss mechanism of magnetic materials and magnetic cores [12]. To this end, Thin Sheet Model (TSM), originated from the statistical energy loss separation developed by Bertotti [13], has been identified as a reliable analytical model to analyse dynamic characteristics of GOES. In this method, the total energy loss  $W_{tot}$  is separated into hysteresis loss  $W_{hys}$ , classical eddy-current loss  $W_{eddy}$ , and excess loss  $W_{exc}$  [14]:

$$W_{tot} = W_{hys} + W_{eddy} + W_{exc} \quad (1)$$

Energy loss mechanism of the material can be accurately analysed based on the static, or quasi-static, and dynamic hysteresis loops, and consequently, energy loss separation of (1) can be described through the magnetic field separation:

$$H(t) = H_{hys}(t) + H_{eddy}(t) + H_{exc}(t) \quad (2)$$

where  $H(t)$  is the magnetic field at the surface of the lamination,  $H_{hys}(t)$  is hysteresis field,  $H_{eddy}(t)$  is eddy current field, and  $H_{exc}(t)$  is excess field.

Two component energy loss model can be also defined and implemented where the materials and associated magnetic cores are subjected to complex magnetising regime [2, 14]. In such circumstances, total energy loss and total magnetic field are separated into hysteresis and dynamic components:

$$W_{tot} = W_{hys} + W_{dyn} \quad (3)$$

$$H(t) = H_{hys}(B) + H_{dyn}(t) \quad (4)$$

Dynamic models based on the three terms and two terms magnetic field separation figures of (2) and (4) have been developed to characterise and energy loss separation of GOESs [14-15]. In a recent publication the two component models of (3) and (4) were further developed to represent the additional energy loss and the corresponding additional magnetic field caused by ILFs in magnetic cores constructed from GOESs [2]:

$$W_{tot} = W_{hys} + W_{dyn} + W_{add} \quad (5)$$

$$H(t) = H_{hys}(B) + H_{dyn}(t) + H_{add}(t) \quad (6)$$

where  $W_{add}$  and  $H_{add}(t)$  are additional energy loss and additional magnetic field caused by the ILFs.

## III. FFT ANALYSIS SOLUTIONS FOR PERIODIC SIGNALS

Fast Fourier Transform (FFT) allows a periodic time domain signal  $f(t)$  to be converted into its equivalent representation in the frequency domain  $F(\omega)$  [16]. The Fourier series of time domain signal  $f(t)$  can be expressed as:

$$f(t) = a_0 + \sum_{n=1}^{+\infty} a_n \cos(n\omega t) + \sum_{n=1}^{+\infty} b_n \sin(n\omega t) \quad (7)$$

where  $\omega = 2\pi f$  is known as the fundamental component or the first harmonic.  $a_0$  is a constant representing the DC component or average value of the signal  $f(t)$  over one period.

Frequency resolution or frequency harmonic of a signal in the frequency domain is an integer multiple of the first harmonic frequency and is given by [16]:

$$f_n = n f_1 \quad n \geq 2 \quad (8)$$

where  $f_1$  is the first harmonic component. Furthermore, the sampling rate of the signal in time domain determines the maximum resolvable frequency in the frequency domain. This frequency is half of the sampling frequency  $f_s$  and given by:

$$f_{max} = \frac{f_s}{2} \quad (9)$$

The sampling frequency  $f_s$ , is determined by the data acquisition system. Therefore, the frequency spectrum, including the first harmonic component, frequency interval and the maximum resolvable frequency, can be determined and controlled based on the time frame duration and sampling frequency of the signal.

#### IV. EXPERIMENTAL SET-UP AND SAMPLE PREPARATION

Experimental works were conducted on 0.3 mm thick Epstein size laminations of 3 % SiFe GOES, with standard grades of M105-30P and a measured resistivity of  $\rho = 0.461 \mu\Omega\text{m}$ . Four stacks, each contains four strips, were assembled and marked as: Stack # 1 with no ILF, Stack # 2 with ILFs at one position, Stack # 3 with ILFs at three positions, and Stack 4 with ILF throughout the laminations. As for the previous work [1, 2], artificial ILFs were applied using lead-free solder. A perspective view of the test samples is shown in Fig 3.

A low frequency magnetising system comprising a single strip tester was employed to magnetise the test samples [15], which is in line with the British standard BS EN 10280:2007 [17]. All test samples were magnetised under controlled sinusoidal induction at a frequency of 50 Hz and peak flux densities from 1.3 T to 1.7 T. According to the guidance provided in the UKAS M3003 [18], Type A and Type B uncertainties of the measuring system were estimated at  $\pm 0.30 \%$  and  $\pm 0.63 \%$ , respectively.

#### V. EXPERIMENTAL RESULTS

Phenomenology of the magnetic hysteresis is a powerful means to characterise magnetic materials and magnetic cores of electromagnetic devices; and therefore, monitoring the DHLs is a reliable approach to understand material behaviour. Comprehending the physical meaning of magnetic hysteresis is a key to understand material behaviour and working principle of electromagnetic devices. In principle, hysteresis phenomenon interpretation can be effectively implemented to understand material behaviour under different magnetisation regimes. This however may not be always a straightforward analysis, as the hysteresis loops may take variety of distinct shapes [12, 19].

##### A. Magnetic hysteresis interpretation:

To start with this study, DHLs and instantaneous waveshapes of magnetic field strength  $H(t)$  of the test samples were initially measured using the test setup outlined in section IV. The results at a magnetising frequency of 50 Hz and peak flux density of 1.7 T, 1.5 T and 1.3 T are shown in Figs 4 and 5, respectively.

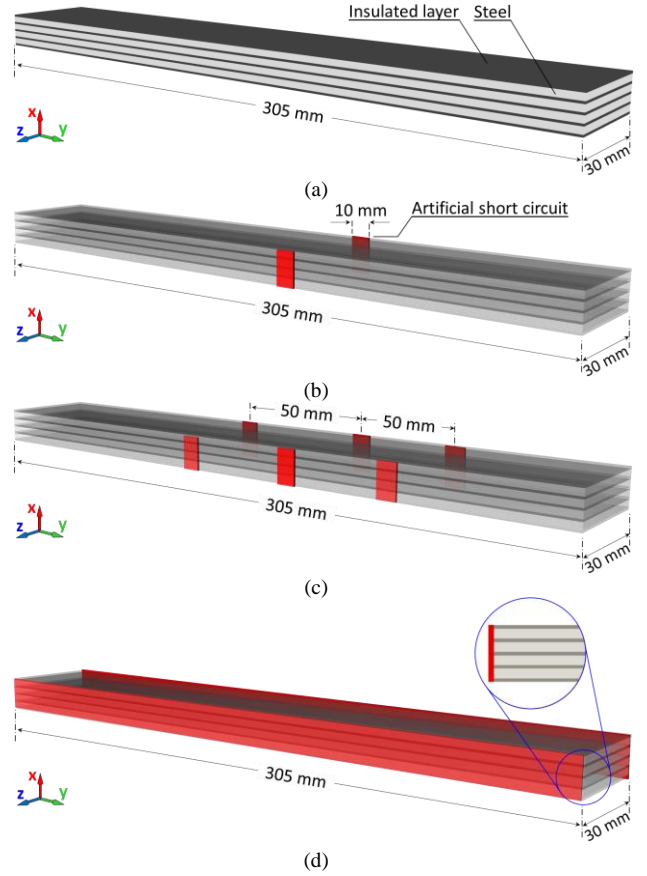


Fig 3 Perspective view of stacks of four laminations (a) without ILF (Stack #1); and with ILFs (b) at one set point (Stack #2) (c) at three set points (Stack #3) and (d) throughout the laminations (Stack #4), (not to scale)

The most noticeable aspect of Fig 4 is the large expansion of the hysteresis loop area, which shows the total energy loss per cycle, and the transformation in the loop shape for various types of ILF. At a given flux density and frequency, important parameters to indicate the soft magnetic properties of the material including coercive field  $H_c$ , peak magnetic field  $H_m$  and residual magnetisation  $B_r$  can be extracted from the measured hysteresis loops. Furthermore, total energy loss per cycle  $W_{tot}$  and relative permeability  $\mu_r$  can be calculated based on the measured hysteresis loops. These are essential parameters to characterise and classify all types of magnetic materials and associated magnetic cores [12, 19]. Based on the measured DHLs, coercive field, peak magnetic field, relative permeability, and total energy loss of the test samples were calculated, the results at a frequency of 50 Hz and peak flux density of 1.7 T, 1.5 T and 1.3 T are shown in Fig 6-a to 6-c, respectively.

These results indicate that, at each particular flux density, ILFs make a major impact on the coercive field  $H_c$  and peak magnetic field  $H_m$ . These facts solidly impact on the total energy loss of the test samples, which is shown in Fig 6 and evidenced from the area of the DHLs of Fig 4. Furthermore, this experiment reveals that relative permeability of the test samples is notably fell off by severity of the ILFs, which is due to the increase in the peak magnetic field strength  $H_m$  at a given peak flux density  $B_m$ . Certainly, this phenomenon is adverse for the overall quality of practical electromagnetic devices.

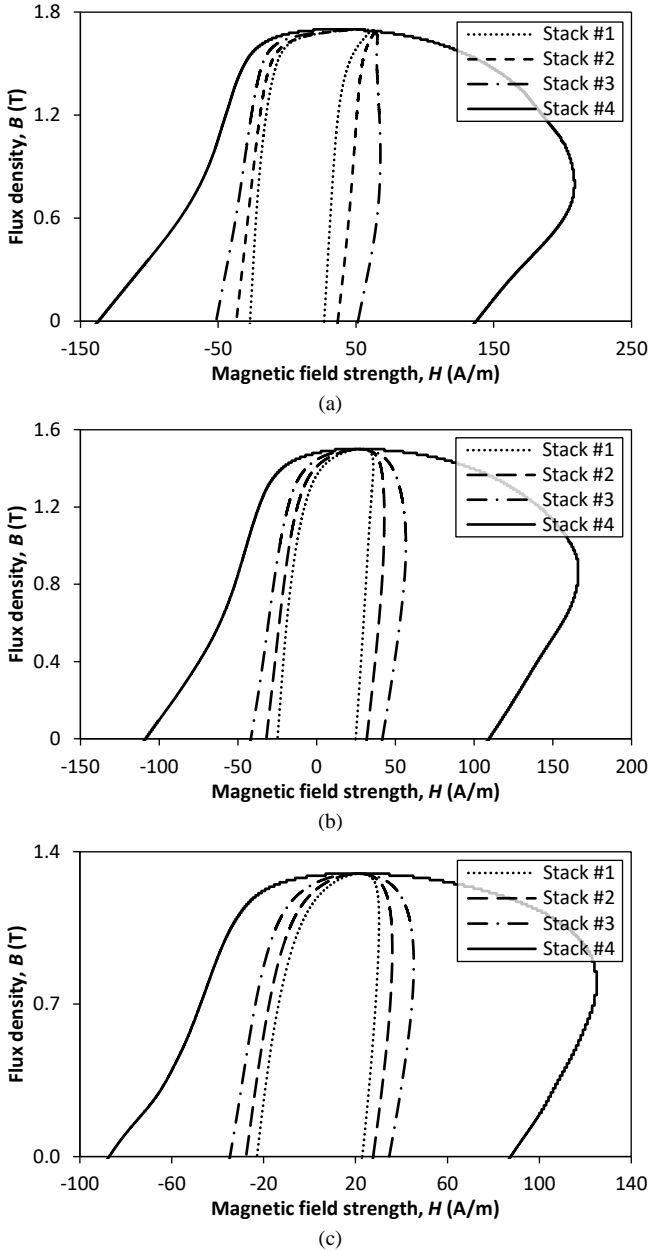


Fig 4 DHLs of the test samples measured at a frequency of 50 Hz and peak flux densities of (a)  $B_{pk} = 1.7$  T, (b)  $B_{pk} = 1.5$  T, and (c)  $B_{pk} = 1.3$  T

More analysis and discussion on quality assessment of the test samples based on the measured DHLs and magnetic field strength can be found in [1-3].

### B. FFT analysis of magnetic field strength:

Magnetic hysteresis is a complex phenomenon, nevertheless, in recent research it was experimentally and analytically demonstrated that ILFs make the magnetising processes even more complicated [1-3], which is evidenced from Figs 4 and 5. Additionally, depends on fault severity, magnetic characteristics including DHLs and instantaneous waveshapes of magnetic field strength of a magnetic core subjected to ILF are far different from the inherent properties of the materials, e.g., what could be measured for a single strip.

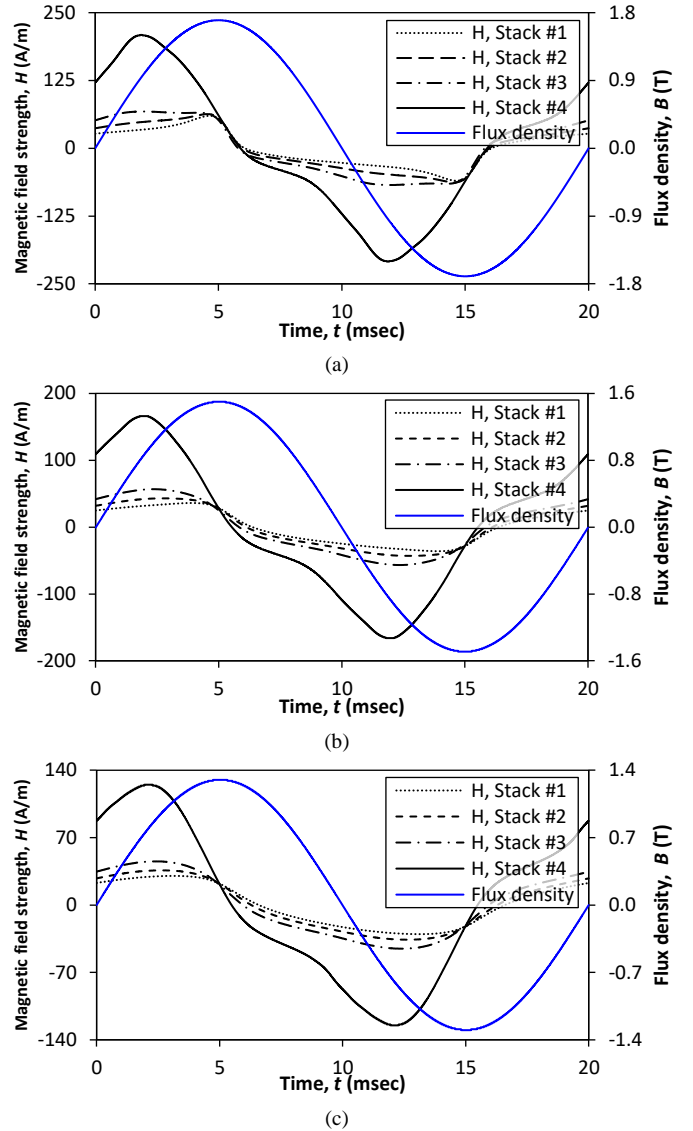


Fig 5 Instantaneous wave shapes  $H(t)$  of the test samples measured at a frequency of 50 Hz and peak flux densities of (a)  $B_{pk} = 1.7$  T, (b)  $B_{pk} = 1.5$  T, and (c)  $B_{pk} = 1.3$  T

All test samples were magnetised under the same flux density  $B(t)$ ; therefore, interpreting the magnetic field strength  $H(t)$  could provide even more information on impacts of the ILFs on the magnetising process. Accordingly, an in-depth analysis on frequency spectrum of the magnetic field strength of the test samples was conducted. Using the magnetising system described in section IV all signals were acquired at a sampling frequency of  $f_s = 500$  kHz. The signals were transformed into frequency domain using FFT function of OriginPro 2021b. Microsoft Excel was also implemented as an auxiliary software, and an interface software was set up to transfer data from Excel to OriginPro and vice versa. In the first stage of this study, magnetic field strength and flux density of Stack #1, without ILF, was transferred into time domain. The instantaneous wave shapes and their frequency spectra in the normalised logarithmic unit decibels (dB) at magnetising frequency of 50 Hz and peak flux density of 1.7 T are shown in Figs 7-a and 7-b, respectively.

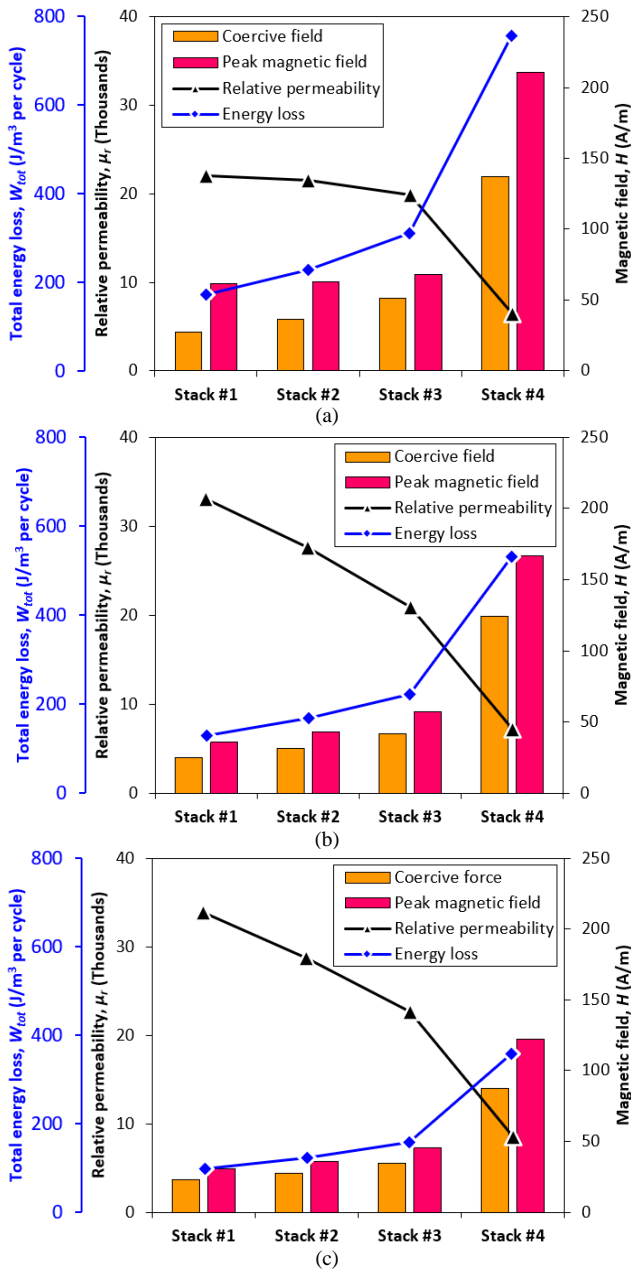


Fig 6 Coercive field, peak magnetic field, relative permeability, and total energy loss per cycle of the test samples at a frequency of 50 Hz and peak flux densities of (a)  $B_{pk} = 1.7 T$  (b)  $B_{pk} = 1.5 T$  and (c)  $B_{pk} = 1.3 T$

As can be seen from Fig 7, the maximum resolvable frequency is  $f_{max} = 250 kHz$ , which is determined by the sampling frequency of the acquired time domain signals as described in section III. Nevertheless, frequency components of higher than  $f > 1600 Hz$  were observed in the spectra of both flux density and magnetic field strength. To identify these frequency components, a pure sine wave of 50 Hz and peak amplitude of 1.7 with the same sampling frequency as for the data acquisition system was generated and its frequency spectrum was calculated. The results are shown and compared with the spectra of the measured  $B(t)$  acquired by the data acquisition in Fig 8.

This result shows that, the high frequency components observed in the flux density and magnetic field strength are

mainly related to the measuring and data acquisition systems. Nevertheless, the frequency range that can be effectively used in this analysis are in the range of  $50 \leq f \leq 1600 Hz$ , as can be seen from Fig 7-b.

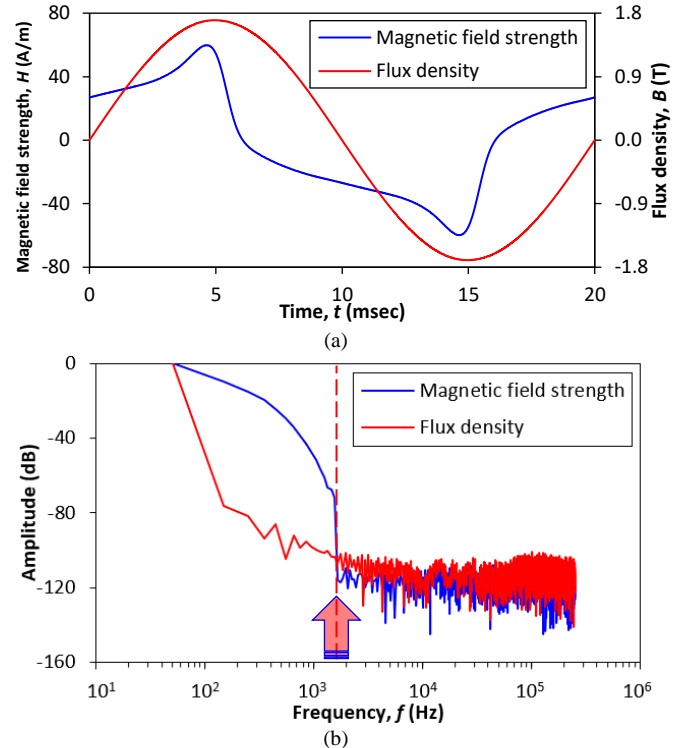


Fig 7 Magnetic field strength and flux density of Stack #1 at a magnetising frequency of 50 Hz and peak flux density of 1.7 T in (a) time domain and (b) frequency domain

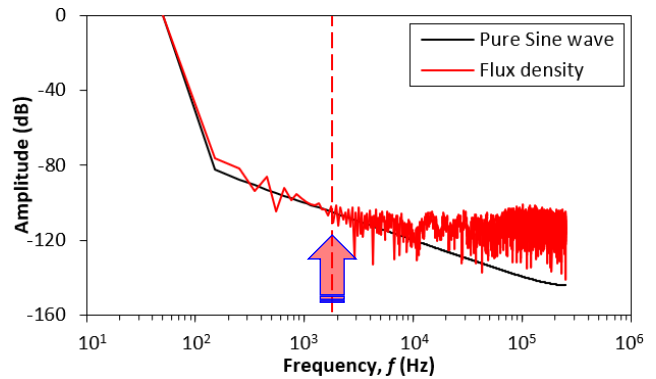


Fig 8 Frequency spectra of a pure sine wave and flux density  $B(t)$  acquired by the magnetising system

In the next step of this study, frequency spectra of the magnetic field strength of the test samples were calculated. During the initial stage of this analysis, it was recognised that frequency spectrum of the magnetic field strength of the test samples, depends highly on the flux density  $B(t)$  which is mainly due to the nonlinear behaviour of the material. The initial results revealed that frequency spectrum analysis at 1.7 T provides a more accurate figure of quality of the test samples. Therefore, this analysis was focused on peak induction of 1.7 T. Fig 9 shows the frequency spectra of magnetic field strength of the test samples at peak induction of 1.7 T.

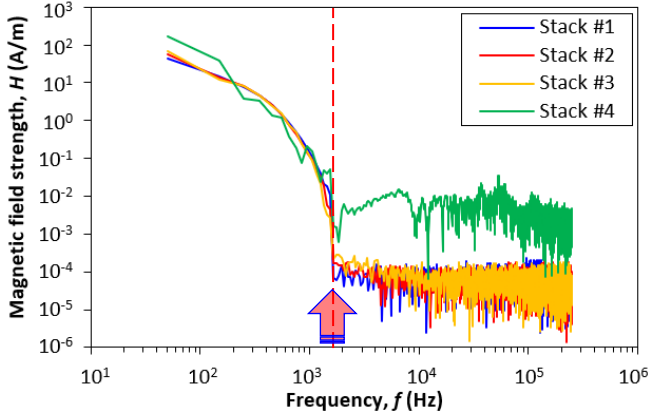


Fig 9 Frequency spectra of magnetic field strength of the test samples at a peak flux density of  $B_{pk} = 1.7 T$

As stated earlier, high frequency components in the magnetic field of Stack #1, without ILF, are mainly related to the magnetic hysteresis and nonlinear properties of the material. Nevertheless, deviation in the amplitude level of the frequency components of Stack #2 to Stack #4 from that of Stack #1 is evident from Fig 9. Furthermore, amplitude level of the frequency components of Stack #2 to Stack #4 changes with severity of the faults for a wide range of frequency between  $50 \leq f \leq 1600 Hz$ . On the other hand, this experiment shows that frequency spectrum of the test samples with ILF remains the same as for Stack #1; however, their amplitudes change with different ILFs. On other word, this experiment revealed that ILFs does not produce any frequency components in the magnetic field strength, and hence in the magnetising current.

To provide more insight on the results, Fig 10 takes a close look at the frequency spectra of magnetic field strength of the test samples for frequency range of  $50 \leq f \leq 1600 Hz$ , with numerical data shown in Table I. Percentage change of each frequency component of magnetic field of the test samples with ILF compared to that of Stack #1 was then calculated using:

$$\% \text{ change} = \frac{H_{fault} - H_1}{H_1} \times 100 \quad (10)$$

where  $H_{fault}$  is magnetic field strength of the test samples with ILF, and  $H_1$  is magnetic field strength of Stack #1. The result is shown in Fig 11.

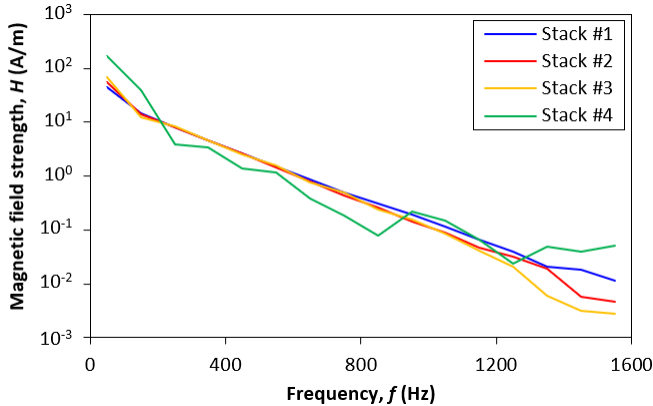


Fig 10 Frequency spectra of magnetic field strength of the test samples at  $B_{pk} = 1.7 T$  and frequency range of  $50 \leq f \leq 1600 Hz$

Table I Numerical data of frequency spectra of magnetic field strength  $H(t)$  at  $B_{pk} = 1.7 T$  and frequency range of  $50 \leq f \leq 1600 Hz$

Frequency, $f$ (Hz)	Magnetic field strength, $H(A/m)$			
	Stack #1	Stack #2	Stack #3	Stack #4
50	43.73	54.84	69.51	169.1
150	14.48	13.77	12.48	38.76
250	7.862	8.016	8.223	3.926
350	4.551	4.500	4.525	3.339
450	2.622	2.573	2.510	1.351
550	1.497	1.427	1.541	1.184
650	0.8731	0.7788	0.7736	0.3889
750	0.4978	0.4379	0.4882	0.1829
850	0.3082	0.2568	0.2405	0.0774
950	0.1886	0.1450	0.1543	0.2158
1050	0.1127	0.0902	0.0863	0.1508
1150	0.0655	0.0472	0.0405	0.0667
1250	0.0394	0.0322	0.0208	0.0236
1350	0.0207	0.0189	0.0060	0.0499
1450	0.0183	0.0057	0.0032	0.0390
1550	0.0113	0.0046	0.0028	0.0508

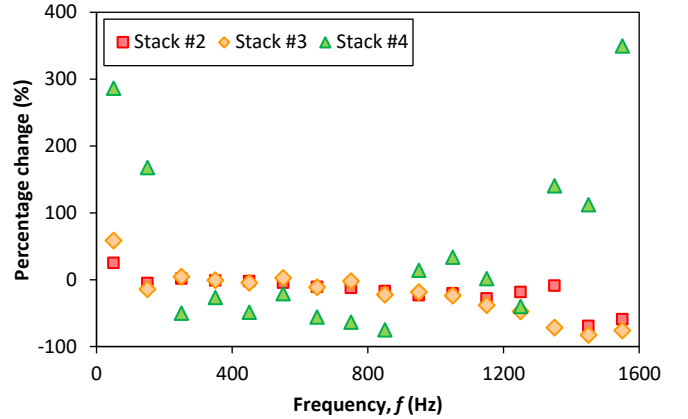


Fig 11 Percentage change of each frequency component of the test samples with ILF compared to that of Stack #1, at  $B_{pk} = 1.7 T$  and frequency range of  $50 \leq f \leq 1600 Hz$

Fig 10 and Table I show that while the fundamental component of the magnetic field strength is notably increased by severity of the ILFs, some higher frequency components are suppressed by ILFs. For example, fundamental component of magnetic field of Stack #4 is increased to 169.1 A/m which is 286.64% higher than that of Stack #1, that is 43.73 A/m. Nevertheless, higher frequency range does not show a rational indication of impacts of core faults on frequency spectrum of magnetic field that can be used in fault classification or diagnosis. Therefore, with reference to these results, condition monitoring of magnetic cores based on the frequency spectrum of the overall magnetic field strength  $H(t)$  may not be a straightforward task.

As stated earlier, the first and immediate impact of ILFs is to create additional eddy current loops, which result in additional localised power loss at the defected zone. In the final stage of this work, frequency spectrum of the additional magnetic field of Stack #2 to Stack #4 were investigated. Considering magnetic field strength of Stack #1 as reference, additional magnetic field of other test samples were calculated using (4) and (6), and their frequency spectrum for the frequency range of  $50 \leq f \leq 1600 \text{ Hz}$  were calculated. The results are shown in Figs 12-a and 12-b, respectively. Numerical data of frequency spectra of additional magnetic field is shown in Table II.

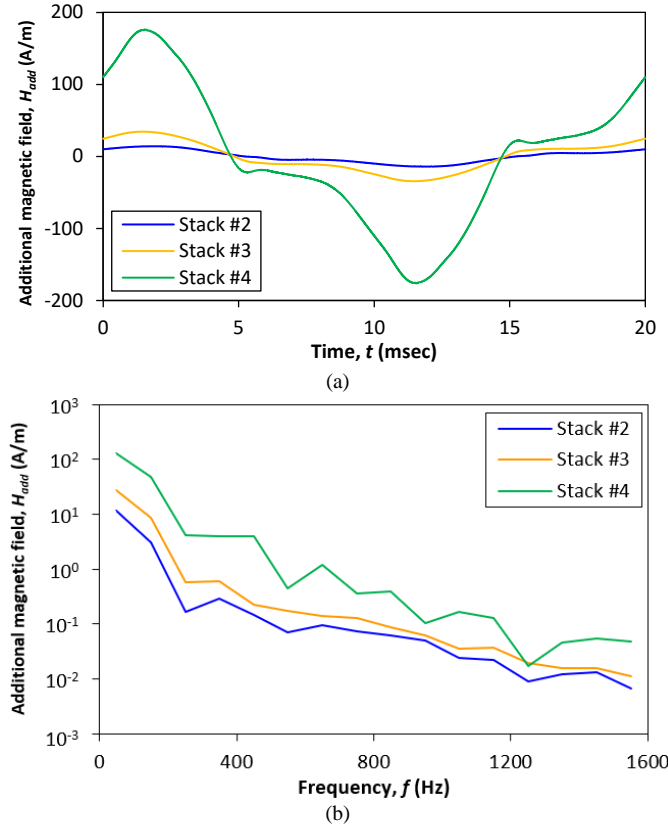


Fig 12 (a) Instantaneous waveshape and (b) Frequency spectrum of additional magnetic field strength  $H_{add}(t)$  at  $B_{pk} = 1.7 \text{ T}$

Unlike frequency spectrum of the overall magnetic field, impacts of ILFs on the frequency spectrum of the additional magnetic field strength  $H_{add}(t)$  can be distinctly observed from Fig 12-b. This implies that, frequency spectrum of  $H_{add}(t)$  carries the information that can effectively be used in core fault detection. Therefore, frequency spectrum analysis of the additional magnetic field strength  $H_{add}(t)$  can be used as an evaluation diagnostic tool to classify core faults and for effective condition monitoring of magnetic cores. These results and associated analysis show that, accurate measurements of DHLs in conjunction with accurate signal processing can provide a reliable tool for effective condition monitoring of magnetic cores of practical e-machines and power transformers.

In the product lines of e-machines and power transformers, the most common technique to assess quality of the magnetic cores is to measure overall power loss, known as no-load loss. The British standard BS EN 60076-1-2011 has defined no-load loss

as “the active power absorbed when a rated voltage (tapping voltage) at a rated frequency is applied to the terminals of one of the windings, the other winding or windings being open circuited” [11]. While this technique requires a basic test setup and interpreting the results is relatively simple, it does not provide a pragmatic figure of quality of the magnetic cores. Therefore, it does not commonly satisfy industry and end users.

Table II Numerical data of frequency spectra of additional magnetic field strength  $H_{add}(t)$  at  $B_{pk} = 1.7 \text{ T}$  and frequency range of  $50 \leq f \leq 1600 \text{ Hz}$

Frequency, $f$ (Hz)	Magnetic field strength, $H_{add}$ (A/m)		
	Stack #2	Stack #3	Stack #4
50	11.80	27.74	127.4
150	3.065	8.390	46.77
250	0.1628	0.5792	4.063
350	0.2843	0.6126	3.886
450	0.1440	0.2279	3.929
550	0.0701	0.1724	0.4367
650	0.0961	0.1410	1.177
750	0.0735	0.1283	0.3621
850	0.0617	0.0888	0.3869
950	0.0489	0.0624	0.1013
1050	0.0239	0.0351	0.1689
1150	0.0221	0.0366	0.1282
1250	0.0091	0.0192	0.0172
1350	0.0120	0.0160	0.0451
1450	0.0134	0.0159	0.0553
1550	0.0067	0.0113	0.0470

Further detailed information on the quality of magnetic cores can be provided by the method suggested in this paper. The proposed approach and associated analysis lay out a reliable platform to study impacts of core faults on magnetising processes of magnetic cores in time and frequency domains. This technique can be further developed for effective quality assessment of magnetic cores in the product line. It can be also used for condition monitoring of e-machines and power transformers during the routine test, at regular intervals, e.g., every 3 to 5 years as recommended in the IEEE Std. 62.2 [20]. For this purpose, a basic schematic diagram associated with a power transformer is proposed and shown in Fig 13.

In this setup, current and potential transformers (CT and PT), measuring system and data acquisition card are used to acquire signals. These signals are then processed to calculate hysteresis characteristics of the magnetic core under test.  $H_1(t)$  is magnetic field strength of a healthy core, which is used as a reference, and  $H_n(t)$  is magnetic field strength of the magnetic core under test. In practice, reference magnetic field  $H_1(t)$  can be obtained from the transformer testing results provided by the manufacturer. These data are usually available in the transformer data sheet and catalogue. Frequency spectrum of  $H_{add}(t)$  is finally calculated using the signal processing unit.

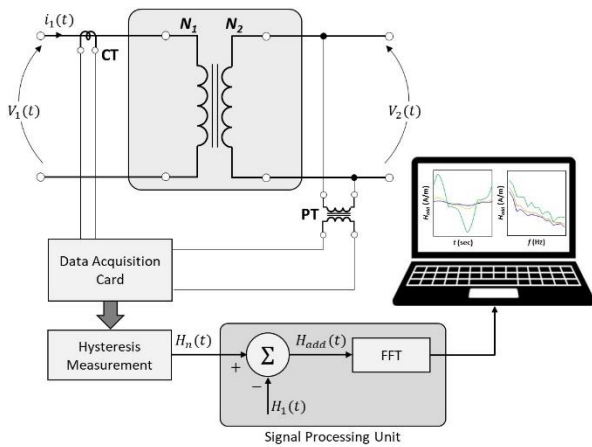


Fig 13 Proposed schematic diagram for condition monitoring of transformer core based on frequency spectrum analysis of magnetic field strength

### CONCLUSION

Electromagnetic devices including e-machines, transformers and reactors are the key players in decarbonised economy and in the battle against the climate change. Exploring new experimental and analytical tools to optimised design, as well as to monitor the operational parameters of electromagnetic devices are crucial to ensure safe and sustainable operation of these devices. This has been an active research area for the academic and industrial researchers, and key requirement for the stakeholders and end users. Practical techniques of fault diagnosis, with high accuracy have been developed and successfully employed for all types of electromagnetic devices. In this respect, Stator Current Signature Analysis (SCSA) can be addressed as a reliable diagnostic technique for condition monitoring of three phase induction motors. Even though the existing techniques are capable of effective fault diagnosis, research and development to improve sensitivity of fault detection, and development of novel techniques to detect weak fault signature is still ongoing.

In series of publications, the author has demonstrated that, interpreting the DHLs and magnetic field strength in time domain is a reliable approach for quality assessment of magnetic cores. While the results are promising, interpreting the acquired signals specifically for minor ILFs may not be a routine task. This work initially aimed to conduct an in-depth analysis on frequency spectrum of the magnetic field strength to identify specific harmonic components caused by ILFs. However, the results showed that, except for the fundamental component, frequency spectrum of the overall magnetic field does not show a rational indication of impacts of core faults. Nevertheless, further analysis revealed that impacts of ILFs can be distinctly observed in the frequency spectrum of the additional magnetic field caused by ILFs. Therefore, with specific emphasis on fault diagnosis in magnetic cores, an accurate signal processing and FFT analysis on the magnetic field strength can provide information on quality of the magnetic cores. This can be used as a diagnostic tool for effective condition monitoring of magnetic cores of practical electromagnetic devices. This information can instruct the design engineers in optimised design of high-quality magnetic cores for modern electromagnetic devices. Furthermore, it helps the maintenance

engineers to identify any potential risk in the magnetic cores and take proper action before they progress into catastrophic failure.

### ACKNOWLEDGMENT

The author is grateful to Cogent Power Ltd. for providing the electrical steels, and Cardiff University for the experimental work. The author is also grateful to EASA, the Electro-Mechanical Authority, for providing Fig 2-b.

### REFERENCES

- [1] H. Hamzehbahmani, "A Phenomenological Approach for Condition Monitoring of Magnetic Cores Based on the Hysteresis Phenomenon," IEEE Transactions on Instrumentation and Measurement, Vol. 70, pp. 1-9, December 2020, Art no. 6003409
- [2] H. Hamzehbahmani, "An Enhanced Analysis of Inter-Laminar Faults in Magnetic Cores with Grain Oriented Electrical Steels for Fault Diagnosis and Condition Monitoring: Theoretical Background and Experimental Verification", IEEE Transaction on Instrumentation and Measurements, Vol. 72, pp. 1-10, March 2023, Art no. 6002610
- [3] H. Hamzehbahmani, "Development of a New Approach to Core Quality Assessment of Modern Electrical Machines", IET Electric Power Applications, Vol. 13, Issue 6, June 2019, pp. 750-756
- [4] K. Liu, S. Wu, Z. Luo, Z. Gongze, X. Ma, Z. Cao, H. Li, "An Intelligent Fault Diagnosis Method for Transformer Based on IPSO-gcForest", Mathematical Problems in Engineering, Vol. 2021, Article ID 6610338, 12 pages, 2021
- [5] W. T. Thomson and I. Culbert, "Current Signature Analysis for Condition Monitoring of Cage Induction Motors: Industrial Application and Case Histories", Wiley-IEEE Press, 2017
- [6] I. Zamudio-Ramirez, R. A. Osornio-Rios, J. A. Antonino-Daviu, H. Razik and R. D. J. Romero-Troncoso, "Magnetic Flux Analysis for the Condition Monitoring of Electric Machines: A Review," IEEE Transactions on Industrial Informatics, Vol. 18, No. 5, pp. 2895-2908, May 2022
- [7] T. Wang, G. Lu and P. Yan, "A Novel Statistical Time-Frequency Analysis for Rotating Machine Condition Monitoring," in IEEE Transactions on Industrial Electronics, Vol. 67, No. 1, pp. 531-541, Jan. 2020
- [8] K. Zhou, C. Yang, J. Liu, Q. Xu, "Dynamic Graph-Based Feature Learning with Few Edges Considering Noisy Samples for Rotating Machinery Fault Diagnosis", IEEE Transactions on Industrial Electronics, Vol. 69, No.10, pp.10595-10604, 2022
- [9] H. Li, Y. Gu, D. Xiang, P. Zhang, P. Yue and Y. Cui, "Online Condition Monitoring of Line-End Coil Insulation for Inverter-Fed Machine by Switching Oscillation Mode Decomposition," IEEE Transactions on Industrial Electronics, Vol. 69, No. 11, pp. 11697-11708, Nov. 2022
- [10] IEEE Std. C37.91, 2000, "IEEE Guide for Protective Relay Applications to Power Transformers", 2000
- [11] BS EN 60076-1-2011, Power transformers - Part 1: General, British Standard, 2012
- [12] G. Bertotti and I. D. Mayergoyz, "The Science of Hysteresis", Academic press, 2005
- [13] G. Bertotti, "General properties of power losses in soft ferromagnetic materials," in IEEE Trans. on Magn., Vol. 24, No. 1, pp. 621-630, Jan. 1988
- [14] S. Zirka, Y. Moroz, S. Steentjes, K. Hameyer, K. Chwastek, S. Zurek and R. Harrison "Dynamic magnetization models for soft ferromagnetic materials with coarse and fine domain structures", Journal of Magnetism and Magnetic Materials, Vol. 394, pp 229-236, Nov. 2015
- [15] H. Hamzehbahmani, "Static Hysteresis Modelling for Grain-Oriented Electrical Steels based on the Phenomenological Concepts of Energy Loss Mechanism", Journal of Applied Physics, Vol. 130, Issue 5, August 2021
- [16] S. Smith, "Digital Signal Processing: A Practical Guide for Engineers and Scientists", Elsevier Science, 2013
- [17] BS EN 10280:2001 + A1:2007, Magnetic Materials - Methods of measurement of the magnetic properties of electrical sheet and strip by means of a single sheet tester, British Standard, 2007
- [18] UKAS M3003, "The Expression of Uncertainty and Confidence in Measurement", Edition 4, Oct 2019
- [19] I. D. Mayergoyz, "Mathematical Models of Hysteresis and Their Applications", Academic press, 2003
- [20] IEEE Standard 62.2-2004, "IEEE Guide for Diagnostic Field Testing of Electric Power Apparatus - Electrical Machinery", June 2005.



**Citation on deposit:**

Hamzehbahmani, H. (2024). Frequency Spectrum Analysis of Magnetic Field Strength for Effective Condition Monitoring of Magnetic Cores. IEEE Transactions on Magnetics, 60(9), 1-9.

<https://doi.org/10.1109/TMAG.2024.3420801> **For final citation and metadata, visit Durham Research Online URL: <https://durham-repository.worktribe.com/output/2773370>**

**Copyright Statement:** This accepted manuscript is licensed under the Creative Commons Attribution 4.0 licence.

<https://creativecommons.org/licenses/by/4.0/>